Beyond cortical geometry: brain dynamics shaped by long-range connections

Jakub Vohryzek [1,2], Morten L. Kringelbach [2,3,4] and Gustavo Deco [1,5]

1. Centre for Brain and Cognition, Computational Neuroscience Group, Department of Information and Communication Technologies, Universitat Pompeu Fabra, Barcelona, Spain
2. Centre for Eudaimonia and Human Flourishing, Linacre College, University of Oxford, UK
3. Department of Psychiatry, University of Oxford, Oxford, United Kingdom
4. Centre for Music in the Brain, Aarhus University, Aarhus, Denmark
5. Institució Catalana de la Recerca i Estudis Avançats (ICREA), Barcelona, Spain

Abstract

A fundamental topological principle is that the container always shapes the content. In neuroscience, this translates into how the brain anatomy shapes brain dynamics. From neuroanatomy, the topology of the mammalian brain can be approximated by local connectivity, accurately described by an exponential distance rule (EDR). The compact, folded geometry of the cortex is shaped by this local connectivity and the geometric harmonic modes can reconstruct much of the functional dynamics. However, this ignores the fundamental role of the rare long-range cortical connections, crucial for improving information processing in the mammalian brain, but not captured by local cortical folding and geometry. Here we show the superiority of harmonics mode combining rare long-range with EDR (EDR+LR) in capturing functional dynamics (specifically long-range functional connectivity and task-evoked brain activity) compared to geometry and EDR representations. Importantly, the orchestration of dynamics is carried out by a more efficient manifold made up of a low number of fundamental EDR+LR modes. Our results show the importance of long-range connectivity for capturing the complexity of functional brain activity through a low-dimensional manifold shaped by fundamental EDR+LR modes.

Introduction

How brain underlying anatomy shapes functional dynamics is an unresolved question being studied from the perspective of network neuroscience[1], brain modelling[7], graph signal theory[8] and neural field theories with different assumptions on the underlying anatomy[3,9]. Therefore,

the choice of underlying anatomical features is of paramount importance in deriving the most simple and parsimonious description of the emerging spatiotemporal brain dynamics.

In previous work on retrograde tract tracing in non-human primates, Kennedy and colleagues have shown that the brain white-matter wiring can be analytically approximated by the Exponential Distance Rule (EDR)[2]. This rule explains the local connectivity of the brain solely in terms of the euclidean distance between points on the cortical surface. And so it follows that the compact, folded geometry of the cortex with its many sulci and gyri is formed by this local connectivity. This corollary implies that the brain anatomical wiring and cortical geometry are the two sides of the same coin and it makes sense to speak of them in agreement. Furthermore, this reflects theoretical work showing that the heat kernel (exponential) is the optimal solution for minimising distance between neighbouring points[10]. Indeed, recent work has suggested that the cortical geometry alone (as a proxy for the underlying anatomical connectivity) can be considered as an important feature driving brain spatiotemporal activity[3,11,12].

However, after deriving the EDR Henry Kennedy famously said; “I am not interested in the EDR itself but mainly the exceptions to the rule”. Indeed, Kennedy and colleagues have shown that in addition to the EDR, the brain possesses a small subset of rare long-range (LR) exceptions to the EDR of brain wiring[4,5]. Furthermore, new evidence using turbulence has demonstrated the fundamental role of the rare long-range anatomical connections in shaping optimal brain information processing[6]. Intuitively, brain cortical foldings defined according to the EDR are indeed the optimal way for brain wiring but they don’t reflect the long-range i.e. it is for example impossible to fold anterior-posterior brain regions in a meaningful way. Therefore, we suggest that the unique contribution of these rare long-range cortical connections changes disproportionately the topological structure of the brain wiring in such a way as to optimise the information processing of the brain. In this work we test this hypothesis that EDR and LR exceptions are fundamental to the parsimonious description of the emerging spatiotemporal dynamics.

In the natural world, a fundamental principle that governs the dynamics of a system constrained by its structure in numerous physical and biological phenomena is the mathematical framework of harmonic modes. Standing wave patterns manifest in many context such as in music with sound-induced vibrations of a guitar string, in physics with the electron wave function of a free particle described by the time-independent Schrödinger equation, or biology with patterns emerging within complex dynamical systems like reaction-diffusion model[13]. The beauty of the mathematical formalism of this phenomenon is that it links in a

single equation, the Helmholtz equation, the specific structure on which the spatiotemporal pattern emerges together with the temporal description in terms of oscillations and spatial description in terms of patterns of synchrony of the standing wave pattern itself.

Here we used Laplacian decomposition of four different graph representations of the underlying anatomy to derive anatomical brain modes: exponential-distance rule (EDR)[2] and long-range exceptions (EDR+LR), geometry-based modes (geometry) and EDR modes (EDR binary and EDR continuous) (Figure 1A). Our results show that EDR+LR achieves significantly better reconstruction of long-range functional connectivity (FC) compared to the other mode representations. Furthermore, pertinent to time-critical information processing, we show that a small subset of modes achieves a disproportionately high reconstruction of task MRI activity. When this subset of modes is considered, EDR+LR achieves better reconstruction for the 47 HCP tasks compared to the other mode representations, suggesting that less is more for information processing in the brain.

Results

EDR+LR reconstructs FC-SC long-range connectivity

To examine how exponential distance rule with long-range exceptions can describe brain activity, we derived the EDR+LR harmonic modes from the EDR matrix fitted to the structural connectome with lambda of 0.162 and added the long-range exceptions to the EDR defined in terms of three standard deviations from a given euclidean distance range larger than 40mm. We constructed the normalised graph laplacian and solved its eigenvalue problem. The eigenvectors of the solution represent the harmonic modes with the eigenvalues sorted in ascending order and reflecting the spatial frequency of the modes with lower modes representing lower spatial frequencies and higher modes representing higher spatial frequencies. Overall, the spatiotemporal activity can be perceived as a weighted contribution of these fundamental bases unfolding over the whole time recording for the spontaneous fMRI or as a weighted contribution of these fundamental bases reconstructing the task-based activations.

One of the features of functional connectivity is the surprisingly high functional connectivity between distant regions[14]. We first investigated to what extent the different anatomical representations reconstruct the long-range connections. These were derived as an intersection of FC connections above 0.5 FC correlations and euclidean distance between the nodes above

40mm (Figure 2A). We then reconstructed these connectivity profiles with an increasing number of modes (1-200) derived from the four representative graphs (Geometry, EDR binary, EDR continuous and EDR+LR) (Figure 2B). The modes are ordered sequentially according to their spatial wavelength represented by their eigenvalues (i.e. mode 1 has the longest spatial wavelength)**.** For all four graphs they monotonically increase the reconstruction correlation reaching on average 0.3 correlation with about 10 modes and by 100 modes reach on average 0.75 correlation before plateauing close to 0.9 correlation on average for the full 200 modes. One noteworthy aspect is that most of the correlation reconstruction happens between 0 and 20 harmonics suggesting that a fairly small number of harmonics is responsible for most of the reconstruction. At 200 modes the EDR+LR outperforms the other spatial basis (Geometry, EDR continuous, EDR binary, paired t-test $p<10^{-4}$).

Less is more - EDR+LR reconstructs task with fewer modes

Using the same approach, we further investigated how well the different bases reconstruct the task-evoked brain activity from 255 healthy HCP participants. We used the 47 task-based contrasts derived from 7 HCP tasks each representing a different activation brain map, and reconstructed them for an increasing number of modes (mode 1-200). For the 7 representative tasks the different bases demonstrate a similar monotonic pattern with steep rise in reconstructed correlation before a slowdown with a near plateau-like behaviour around 200 modes and reconstructed correlation values exceeding 0.9 for most of the bases and tasks (Figure 3A Top). To analyse the reconstruction pattern, we computed the FC correlation contribution of a given mode when added to the reconstruction. This demonstrates that the apparent bulk of the reconstruction is being obtained from a relatively small number of modes 0-20 in comparison to the rest (Figure 3A Bottom). This shows that reconstructing both spontaneous and task-evoked activity is represented in a very small space of 0-20 modes, suggesting that both types of dynamics, spontaneous and task-evoked, lie in a lower-dimensional manifold. Focusing only on the first 20 modes, we examined how the 47 task-evoked activations maps are reconstructed in comparison to the geometric modes. On average EDR+LR showed the most accurate reconstruction across tasks and number of reconstructed modes 1-20 with EDR binary and EDR continuous being on an equal footing with the geometric modes (Figure 3B). By construction, the modes span an orthogonal basis set in which the individual mode contributions are mapped to. To motivate the neatness and accuracy of reconstructing the activation maps with as little EDR+LR as possible, we visually demonstrate

the reconstruction of relational tasks for 5, 10, 15 and 20 modes showing the indistinguishable similarity to the activation map itself (Figure 3D). Moreover, it is not surprising that the EDR+LR basis, due to their unique topology, reconstruct with fewer modes more accurately the tasks as it can be appreciated in the motor tasks where more nuanced features are picked up in comparison to the geometric modes (Figure 3E).

Discussion

The unique mathematical formulation of harmonic modes links the description of how structure gives rise to the emerging spatiotemporal activity of brain dynamics. We show that EDR+LR modes have the highest reconstruction correlation for an increasing number of modes when describing the FC long-range connections of spontaneous fMRI activity. Furthermore, for the reconstruction of the 7 activation task fMRI maps lower frequency modes contribute disproportionately more toward the reconstruction error. We therefore reconstructed the error for the 47 HCP tasks benchmarked against the geometrical modes for the first 20 modes. On average EDR+LR showed the most accurate reconstruction across tasks and number of reconstructed modes 1-20. Our results demonstrate the importance of long-range connectivity as a key feature of shaping brain functional activity both for the spontaneous and task-based fMRI. Moreover, functional brain activity is shown to be on a lower-dimensional manifold span by a subset of these fundamental modes with the most appropriate representation from the EDR+LR graph, suggesting that less is more for efficient information processing in the brain.

In both spontaneous and task-based reconstruction cases, the EDR+LR demonstrate high reconstruction only with a subset of modes from its harmonic repertoire. Despite the superior performance of the EDR+LR harmonic modes, it is remarkable that the other harmonic bases, geometric and EDR-based, performed strongly as well. This reflects a fundamental insight where large-scale brain organisation can be described as lying in a low-dimensional manifold. This in part can be explained by the brain's coordinated cognition and behaviour which cannot happen without integrative tendencies of its underlying dynamics. Indeed, brain dynamics operating in a reduced number of dimensions has been shown to predict more effectively the brain's behaviour[15]. As such one can talk of brain activity as a flow on this low dimensional manifold embedded in the space of these relatively few harmonic modes[16].

One of the fundamental considerations is what type of brain's dynamics we wish to reconstruct. Unlike the traditional approach where the whole static functional connectivity is reconstructed[3], we focused on reconstructing the most salient features of the brain's

spontaneous fMRI activity, namely the functionally strong long-range connection. Our work underscores the cardinal role of long-range connectivity in cognitive processing and advocates for prioritising the reconstruction of exceptional connections over exhaustive coverage of the entire functional connectivity matrix. Moving beyond, it is important to consider temporally evolving descriptions of brain dynamics as recent work has demonstrated the relevance of dynamics in understanding brain function and its related pathologies[17]. Moreover, many whole-brain modelling techniques have been suggesting the need to consider further descriptors of brain activity that goes beyond the static FC description[18]

In this work, we derived both EDR binary and EDR continuous harmonic modes. These reflect different methodological considerations when calculating the laplacian eigenmaps [10]. We have applied the continuous form of the graph laplacian on the EDR (EDR continuous) showing that this simple change improves the reconstruction accuracy by about 0.02 correlation to the binarized version (EDR binary) making it practically on the same footing as the geometric bases. It is therefore warranted to unify the methodological approaches before comparing the superiority of the different anatomical features as the differences might be simply explained by methodological choices themselves. Therefore we caution future research to unify the applied methodologies in this direction.

Methods

Experimental Data

HCP Functional MRI

We used the publicly available Human Connectome Project (HCP) dataset, Principal Investigators: David Van Essen and Kamil Ugurbil: 1U54MH091657) with the funding coming from sixteen NIH Institutes and Centres supporting the NIH Blueprint for Neuroscience Research; and by the McDonell Centre for Systems Neuroscience at Washington University. All participants joined voluntarily and provided informed consent. The open-access data used in this study were obtained through the WU–Minn HCP consortium, following approval from the local ethics committee. The data were shared with the authors in accordance with the terms specified by the HCP for data usage. All procedures conducted in this study adhered to the protocols outlined in these data use terms. For a comprehensive description of the image acquisition protocol, preprocessing pipelines[19], and ethics oversight, please refer to the detailed account provided[19,20].

Spontaneous fMRI dataset

We used the spontaneous fMRI dataset from the freely accessible database with connectome DB account at https://db.humanconnectome.org. Timeseries were minimally processed. Consistent with the Pang et al. 2023, we used a subset of 255 participants (22-35yo, 132 F and 123 M) who completed all spontaneous and tasks-based fMRI recordings, further excluding twins and siblings. The neuroimaging acquisition was carried out on a 3-T connectome-Skyra scanner (Siemens). A single spontaneous fMRI acquisition, lasting approximately 15 minutes, was conducted on the same day. During this session, participants kept their eyes open with relaxed fixation on a projected bright crosshair against a dark background. The HCP website offers comprehensive details on participant information, acquisition protocols, and data preprocessing for both spontaneous and the seven tasks. In summary, the data underwent preprocessing using the HCP pipeline, which employs standardised methods with FSL (FMRIB Software Library), FreeSurfer, and Connectome Workbench software. This standardised preprocessing encompassed correction for spatial and gradient distortions, head motion correction, intensity normalisation, bias field removal, registration to the T1-weighted structural image, transformation to the 2-mm MNI space, and application of the FIX artefact removal procedure. Head motion parameters were regressed out, and structured artefacts were removed using independent component analysis, followed by FMRIB's ICA-based X-

noiseifier (ICA+FIX) processing. The preprocessed time series for all grayordinates were in the HCP CIFTI grayordinates standard space, available in the surface-based CIFTI file for each participant during spontaneous fMRI.

Tasks-based fMRI dataset

For the task-based fMRI analysis, we obtained fMRI data from 7 distinct task domains known to reliably engage a diverse range of neural systems[3,19]. The tasks included were social, motor, gambling, working memory (WM), language, emotion, and relational. We used the specific contrasts within each task domain, highlighting the key contrast investigated in this study. These contrasts were provided by[3] from https://osf.io/xczmp/ in "S255_tfMRI_ALLTASKS_raw_lh" .mat file. In total, the analysis encompassed 47 contrasts, incorporating the 7 key contrasts. In brief, the analysis was performed on individual task-activation maps generated through FSL's cross-run (Level 2) FEAT analysis[21]. The task maps, provided by the Human Connectome Project (HCP), were used with minimal smoothing (2 mm), and mapped onto the fsLR-32k CIFTI space. This mapping was achieved using multimodal surface matching, resulting in a representation of each individual's task data (32,492 vertices in each hemisphere). Additional information about each task and contrast as well as further details on the data can be found[3,19].

fMRI parcellation

A custom MATLAB script, utilising the 'ft_read_cifti' function from the Fieldtrip toolbox, was employed to extract the average time series of all grayordinates in each region defined by the Glasser360 parcellations (180 regions per hemisphere) in the HCP CIFTI grayordinates standard space. For each hemisphere the vertex-space to ROI-space meant going from 32,492x1200 to 180x1200 for spontaneous fMRI and 32,492x1 to 180x1 for task-based fMRI. Consistent with Pang et al. (2023) our analysis focused on the left hemisphere only.

HCP Diffusion MRI

To obtain the structural connectivity for the fitting of the EDR and derivation of long-range exceptions to the EDR, we used the high-resolution connectivity maps from dMRI tractography[22]. These were provided by[3] in "S255_high-resolution_group_average _connectome_cortex_nomedial-lh" .mat file. In brief, the connectome was derived by estimating the connectivity of each of the 32,492 vertices within the cortical surface mesh by tracing streamlines from each point until they terminated at another point. Connection weights

between vertices, treated as nodes, were determined as the number of interconnecting streamlines without normalisation[23]. The dMRI tractography was conducted on individuals from the Human Connectome Project (HCP). Subsequently, the individual weighted connectivity matrices were combined, each of size 32,492 × 32,492, to generate a group-averaged connectome. The weights in this connectome represented the average number of streamlines, providing a comprehensive depiction of group-level connectivity. Further details can be found in[3].

Structural MRI

For the fitting of the EDR, we used the euclidean distance between the vertices of the cortical mesh representation for the left hemisphere (32,492x32,492). This mesh was derived from the FreeSurfer's fsaverage population-averaged template available on github.com/ThomasYeoLab/ CBIG/tree/master/ data/templates/surface/fs_LR_32k. It is to be noted, we used the version provided by[3] in the "fsLR_32k_midthickness-lh" .vtk file.

Exponential Distance Rule (EDR)

Previous work has demonstrated that the brain white-matter wiring, based on retrograde tract tracing in non-human primates, can be analytically approximated by the Exponential Distance Rule (EDR) [2]. Here, we derived the Exponential Distance Rule of the underlying human anatomy using diffusion MRI. Mathematically, the exponential distance rule can be described with exponential decay function as follows:

$$C_{i,j}^{EDR} = Ae^{-\lambda(r(i,j))}$$

where r(i,j) is the euclidean distance between vertices i and j and λ is the decay. By fitting the exponential function to the dense connectome, we set A= 0.066 and λ = 0.162 mm^{-1} where lambda is consistent with previous literature[4,6].

Relationship to Belkin and Niyogi

The exponential distance rule, as an optimal solution for connecting distance-separated brain regions in the brain, can also be intuitively understood from first principles. Belkin and colleagues have analytically shown the relationship between graph Laplacian, Laplace Beltrami Operator and the heat kernel which is the optimal solution for locality preservation -

formally as $W_{ij} = e^{\frac{-\left\|x_i - x_j\right\|^2}{t}}$ where t is the decay parameter of the heat kernel[10]. It can thus be appreciated that this equation also follows exponential decay (gaussian) similar to the EDR.

Harmonic Modes

In this work, we used four different types of graph representations to describe various aspects of anatomical features or methodological approaches. Namely, we carried out the analysis on what we call Geometric, EDR binary, EDR continuous and EDR+LR modes. In what follows, we describe the remaining three types of harmonic modes representations.

EDR binary: For the EDR binary, we use the EDR with the same parameters as in Pang et al. (2023) to define the weight of a given edge between vertices i and j. In other words, the weight is determined by the euclidean distance between regions i and j and the fitted lambda parameter, λ = 0.12 mm^{-1} (see section Exponential Distance Rule). Then, as in Pang et al. (2023), we created a binary adjacency matrix where nodes i and j are retained and binarised only if the weight strength surpasses randomly distributed distribution of the weights. This option results in a binary adjacency matrix whereby $C_{ij} = 1$ if i and j are above randomly distributed distribution of the weights and $C_{ij} = 0$ if i and j are below the randomly distributed distribution of the weights. The choice of this approach was motivated to stay consistent with previous work by Pang et al. (2023) in order for the results to be directly comparable.

EDR continuous: For the EDR continuous, we similarly use the EDR with the same parameters to define the weight of a given edge between vertices i and j using the EDR with λ = 0.12mm^{-1}. Unlike the thresholding in EDR binary (applied in Pang et al. (2023)) where connections are retained and binarised if they surpass connection weights from a randomly derived distribution , here all the connections and their weights are kept. This option results in a weighted adjacency matrix whereby $W_{ij} = Ae^{-\lambda(r(i,j))}$. Furthermore, we argue in this paper that this detailed explanation between EDR binary and EDR continuous adjacency matrices is warranted as it zeroes in on what is an appropriate comparison between graph laplacian and continuous Laplace-Beltrami analysis and we motivate future comparative research in this direction.

Geometry: The geometric modes were calculated using the Laplace Beltrami Operator (LBO) on the cortical mesh. We used the publicly available version from previously published work which can be downloaded from https://osf.io/xczmp/ in "fsLR_32k_midthickness-lh_emode_200" .txt file[3]. In brief, the LBO is in general defined as follows:

$$\Delta := \frac{1}{W}\Sigma_{i,j}\frac{\delta}{\delta x_i}(g^{ij}W\frac{\delta}{\delta x_j}),$$

With g^{ij} being the inverse of the inner product metric tensor $g_{ij} := <\frac{\delta}{\delta x_i}, \frac{\delta}{\delta x_j}>$, $W := \sqrt{\ }det(G)$ and $G := (g_{ij})$. The solution of the eigenvalue problem was implemented in a python package LaPy using the cubic finite element method[24]. For further details consult[3]. Although not explicitly stated, the derivation leverages an exponential kernel that is reminiscent of the EDR.

EDR+LR: Previous research has shown that human as well as non-primate anatomy is characterised by a relatively small proportion of long range outliers to the EDR[4,6]. Therefore for the EDR continuous adjacency matrix we wanted to implement a version where these long-range (LR) exceptions are taken into account. Using the structural connectivity matrix, we computed the binned distribution (400 bins) as a function of euclidean distance. We defined connectivity exceptions as 3 standard deviations above the mean for a given distance bin that are longer than 40mm. To derive the EDR+LR connectivity matrix we combine the EDR continuous with LR exceptions to the EDR.

EDR+LR relationship to Connectome Harmonics

Combining short-range and long-range connectivity can be performed in many ways. Indeed our previous work on connectome harmonics has defined the anatomical connectivity in terms of short-range, nearest-neighbour connections on the cortical surface, combined together with long-range connections, derived from the diffusion MRI in terms of the connectome[9]. In this light, here, we derive the short range connections in a more principled way through the "EDR continuous" while accounting for the long-range connections in terms of the exceptions to the EDR as stated above. Furthermore, we avoid binarization of the adjacency matrix for the calculation of the laplacian as it has shown to retain important information in the reconstruction of both spontaneous and task-evoked fMRI from our results on binary and continuous EDR brain modes.

.

Laplacian Decomposition

Having derived the EDR+LR, EDR binary and EDR continuous adjacency matrix, we calculated the normalised graph Laplacian as

$$L^{norm} = D^{-1/2} L D^{-1/2}$$

with $L = D - A$ where D is the diagonal degree matrix defined as $D = \sum_{i=1}^{n} A(i,j)$. Finally, the harmonic modes were computed as eigenvectors of the following eigenvalue problem

$$\Delta_A \psi_k(x_i) = \lambda \psi_k(x_i) \ , \forall x_i \in \upsilon$$

with $\lambda_k, k \in 1, \ldots, n$ are the eigenvalues of Δ_A and ψ_k is the k^{th} harmonic mode.

Decomposition of brain activity with harmonic modes

We can represent the spatiotemporal spontaneous fMRI recording and the activation maps of task-based fMRI as a weighted contribution of the harmonic modes as follows

$$F(x,t) = \sum_{k=1}^{N} a_k(t) \psi_k(x)$$

Where F is the spatiotemporal timercordings for each subjects with dimension 32,492x1200 (x,t), $a_k(t)$ has dimension 1x1200 and is the contribution of k^{th} harmonic to the F timecourse at time t. Note that for the purely spatial data of task-based fMRI the same applies except of the contributions being independent of time ie $a_k(t) \rightarrow a_k$. Both in spontaneous and task-based fMRI, the contributions are computed as the inner product between the spatial patterns and harmonic modes

$$a_k(t) = < F(x,t), \psi_k(x) >.$$

Reconstruction error

To compare both the spontaneous and task-based empirical fMRI data with the reconstructed data with a subset of harmonic modes, we first parcellated the data to Glasser360 parcellation (we focused on the left hemisphere resulting in 180 nodes). For the spontaneous fMRI, we calculated the interregional functional connectivity (FC -180x180) and focused on the most salient features by reconstructing the long-range functional connectivity derived as a subset of connections with high-correlation values (> 0.5 correlation) and a long euclidean distance (> 40mm). Then, we calculated the reconstruction error as the Pearson's correlation between the empirical and reconstructed long-range functional connectivity. For the task-based fMRI we

calculated the reconstruction error as the Pearson's correlation between the empirical and reconstructed activation maps.

Acknowledgements

Jakub Vohryzek is supported by EU H2020 FET Proactive project Neurotwin grant agreement no. 101017716, Morten L. Kringelbach is supported by the European Research Council Consolidator Grant: CAREGIVING (615539), Pettit Foundation, Carlsberg Foundation and Center for Music in the Brain, funded by the Danish National Research Foundation (DNRF117). Gustavo Deco is supported by the Spanish Research Project PSI2016-75688-P (Agencia Estatal de Investigación/Fondo Europeo de Desarrollo Regional, European Union); by the European Union's Horizon 2020 Research and Innovation Programme under Grant Agreements 720270 (Human Brain Project [HBP] SGA1) and 785907 (HBP SGA2); and by the Catalan Agency for Management of University and Research Grants Programme 2017 SGR 1545.

Author contributions

J.V. contributed to conceptualization, formal analysis, investigation; methodology, software, writing original draft, reviewing editing. M.L.K contributed to conceptualization, writing, supervision, reviewing and editing. G.D. contributed to conceptualization, formal analysis, investigation, software, supervision, writing, reviewing and editing.

Competing interests.

All authors report no conflict of interest.

References

1. Bullmore, E. & Sporns, O. Complex brain networks: graph theoretical analysis of structural and functional systems. *Nat. Rev. Neurosci.* **10**, 186–198 (2009).
2. Ercsey-Ravasz, M. *et al.* A predictive network model of cerebral cortical connectivity based on a distance rule. *Neuron* **80**, 184–197 (2013).

3. Pang, J. C. *et al.* Geometric constraints on human brain function. *Nature* **618**, 566–574 (2023).
4. Markov, N. T. *et al.* The role of long-range connections on the specificity of the macaque interareal cortical network. *Proc. Natl. Acad. Sci. U. S. A.* **110**, 5187–5192 (2013).
5. Markov, N. T. *et al.* Cortical high-density counterstream architectures. *Science* **342**, 1238406 (2013).
6. Deco, G. *et al.* Rare long-range cortical connections enhance human information processing. *Curr. Biol.* **31**, 4436–4448.e5 (2021).
7. Breakspear, M. Dynamic models of large-scale brain activity. *Nat. Neurosci.* **20**, 340–352 (2017).
8. Preti, M. G. & Van De Ville, D. Decoupling of brain function from structure reveals regional behavioral specialization in humans. *Nat. Commun.* **10**, 1–7 (2019).
9. Atasoy, S., Donnelly, I. & Pearson, J. Human brain networks function in connectome-specific harmonic waves. *Nat. Commun.* **7**, 1–10 (2016).
10. Belkin, M. & Niyogi, P. Laplacian eigenmaps for dimensionality reduction and data representation. *Neural Comput.* **15**, 1373–1396 (2003).
11. Pang, J. C. *et al.* Reply to: Commentary on Pang et al. (2023) Nature. *bioRxiv* 2023.10.06.560797 (2023) doi:10.1101/2023.10.06.560797.
12. Faskowitz, J. *et al.* Commentary on Pang et al. (2023) Nature. *bioRxiv* 2023.07.20.549785 (2023) doi:10.1101/2023.07.20.549785.
13. Atasoy, S., Deco, G., Kringelbach, M. L. & Pearson, J. Harmonic Brain Modes: A Unifying Framework for Linking Space and Time in Brain Dynamics. *Neuroscientist* (2017) doi:10.1177/1073858417728032.
14. Fox, M. D. *et al.* The human brain is intrinsically organized into dynamic, anticorrelated

functional networks. *Proceedings of the National Academy of Sciences* **102**, 9673–9678 (2005).

15. Perl, Y. S. *et al.* Whole-brain modelling of low-dimensional manifold modes reveals organising principle of brain dynamics. *bioRxiv* 2023.11.20.567824 (2023) doi:10.1101/2023.11.20.567824.
16. Vohryzek, J. *et al.* Harmonic decomposition of spacetime (HADES) framework characterises the spacetime hierarchy of the DMT brain state. *bioRxiv* 2023.08.20.554019 (2023) doi:10.1101/2023.08.20.554019.
17. Preti, M. G., Bolton, T. A. & Van De Ville, D. The dynamic functional connectome: State-of-the-art and perspectives. *Neuroimage* **160**, 41–54 (2017).
18. Vohryzek, J., Cabral, J., Vuust, P., Deco, G. & Kringelbach, M. L. Understanding brain states across spacetime informed by whole-brain modelling. *Philos. Trans. A Math. Phys. Eng. Sci.* **380**, 20210247 (2022).
19. Barch, D. M. *et al.* Function in the human connectome: task-fMRI and individual differences in behavior. *Neuroimage* **80**, 169–189 (2013).
20. Van Essen, D. C. *et al.* The WU-Minn Human Connectome Project: an overview. *Neuroimage* **80**, 62–79 (2013).
21. Woolrich, M. W., Behrens, T. E. J., Beckmann, C. F., Jenkinson, M. & Smith, S. M. Multilevel linear modelling for FMRI group analysis using Bayesian inference. *Neuroimage* **21**, 1732–1747 (2004).
22. Mansour L, S., Tian, Y., Yeo, B. T. T., Cropley, V. & Zalesky, A. High-resolution connectomic fingerprints: Mapping neural identity and behavior. *Neuroimage* **229**, 117695 (2021).
23. Tournier, J.-D. *et al.* MRtrix3: A fast, flexible and open software framework for medical image processing and visualisation. *Neuroimage* **202**, 116137 (2019).

24. Laplace–Beltrami spectra as ‘Shape-DNA’ of surfaces and solids. *Comput. Aided Des. Appl.* **38**, 342–366 (2006).

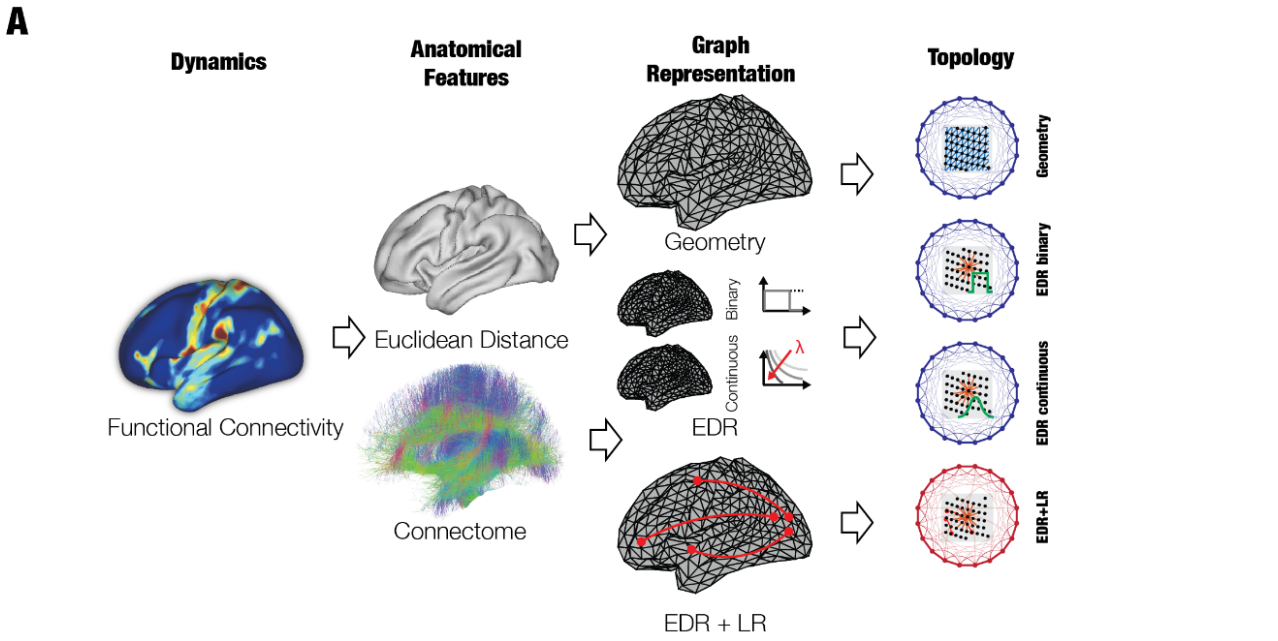
A
Dynamics
Anatomical Features
Graph Representation
Topology
Functional Connectivity
Euclidean Distance
Connectome
Geometry
Binary
Continuous
EDR
EDR + LR
Geometry
EDR binary
EDR continuous
EDR+LR

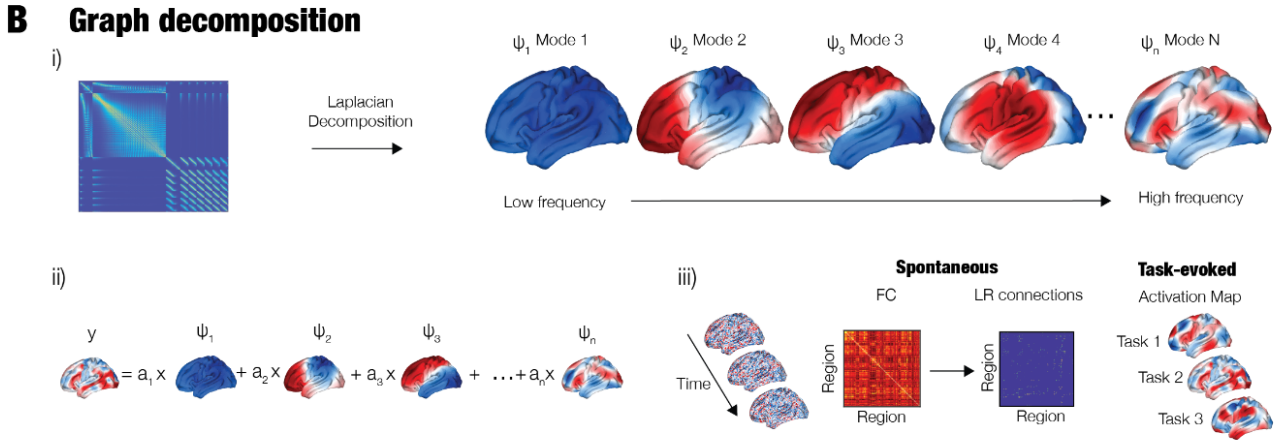
B Graph decomposition
i)
Laplacian Decomposition
Mode 1
Mode 2
Mode 3
Mode 4
Mode N
Low frequency
High frequency
ii)
iii)
Spontaneous
FC
LR connections
Task-evoked
Activation Map
Time
Region
Task 1
Task 2
Task 3

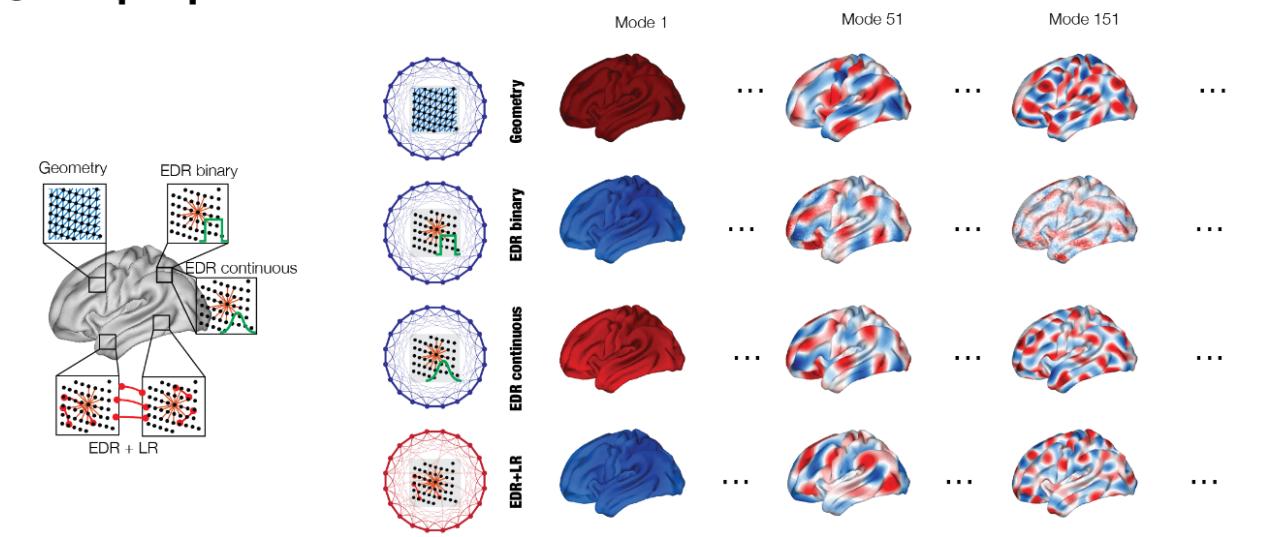
C Graph representation
Geometry
EDR binary
EDR continuous
EDR + LR
Mode 1
Mode 51
Mode 151
Geometry
EDR binary
EDR continuous
EDR+LR


D Reconstructing Long-Range Connections
LR Connections
Region
Region
Correlation
EDR binary
EDR continuous
Geometry
EDR+LR
E Minimal modes used in reconstructing task
FC correlation contribution
Modes

Figure 1. The crucial role of long-range connectivity for accurately describing whole-brain dynamics. A) The functional dynamics measured with fMRI emerge from the underlying anatomical structural connectivity which can be represented as graphs. Here, we study the four main graph representations: 1) geometrical modes (Pang et al. 2023); 2) exponential distance rule (EDR, binarised); 3) EDR (continuous) and 4) EDR with long-range exceptions (EDR+LR). **B)** With regards to the graph representations, i) the different modes are derived from applying the laplace decomposition on the graph representation by solving the eigenvalue problem. The different modes are in ascending spatial frequency. ii) These modes are used to reconstruct the fMRI activity by a linear combination of their contributions. iii) This is used to reconstruct the spontaneous fMRI activity and in particular the functional long-range connectivity exceptions (derived as high-correlation values, >0.5 correlation, and over a long euclidean distance, >40mm, see *Methods*), as well as all the 47 task fMRI activation maps. **C)** The four different graph representations were constructed and decomposed into their associated modes. Note that the EDR modes all use a lambda parameter of $0.162mm^{-1}$, which is coming from the fitting of the empirically derived connectome. **D)** Demonstrating the importance of long-range connections, EDR+LR achieves a superior reconstruction of long-range fMRI connectivity compared to geometric, EDR (binary) and EDR (continuous) graph representations. **E)** Equally important, the EDR+LR needs fewer modes to reconstruct task data compared to the three other graph representations, demonstrating the importance of long-range connectivity.[3] Parts of the figures have been modified from Pang et al. (2023).

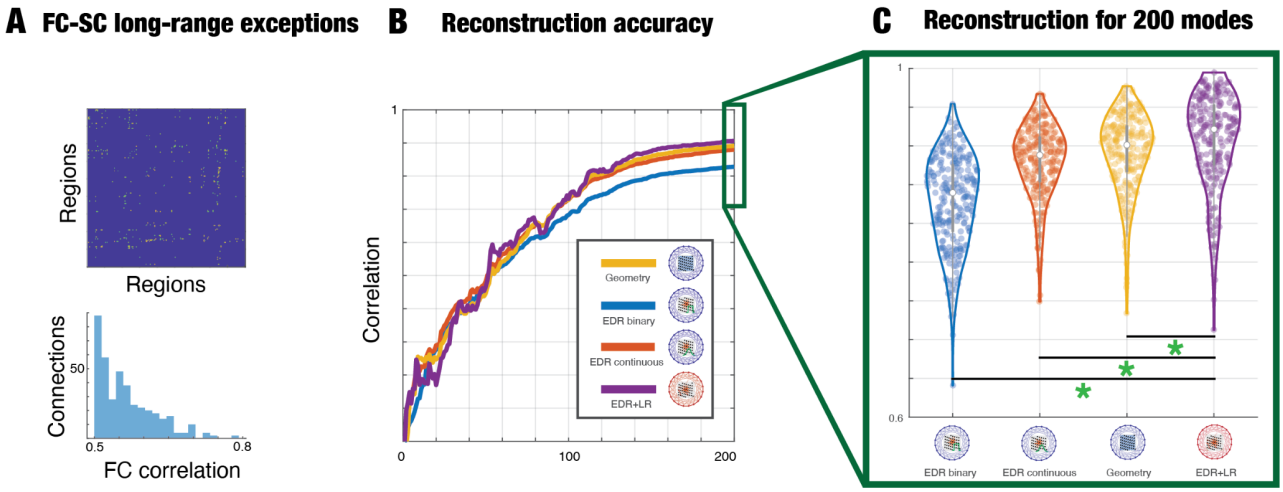

Figure 2. Better reconstructions of brain dynamics are found with EDR and rare long-range exceptions in the graph representation. A) One of the most important features of cortical dynamics are long-range functional connections (defined by high correlation values, >0.5 correlation, and Euclidean distance, >40mm). **B)** EDR+LR outcompetes the other graph representations as shown by the reconstruction of FC long-range connections for an increasing number of modes (1-200) for the four representative graph representations. The individual lines show the average across all 255 HCP participants. **C)** EDR+LR is significantly better than the other graph representations when using a reconstruction with 200 modes as shown by the average result for the correlation values across all the 255 HCP subjects (paired t-test $p<10^{-4}$). Parts of the figures have been modified from Pang et al. (2023).

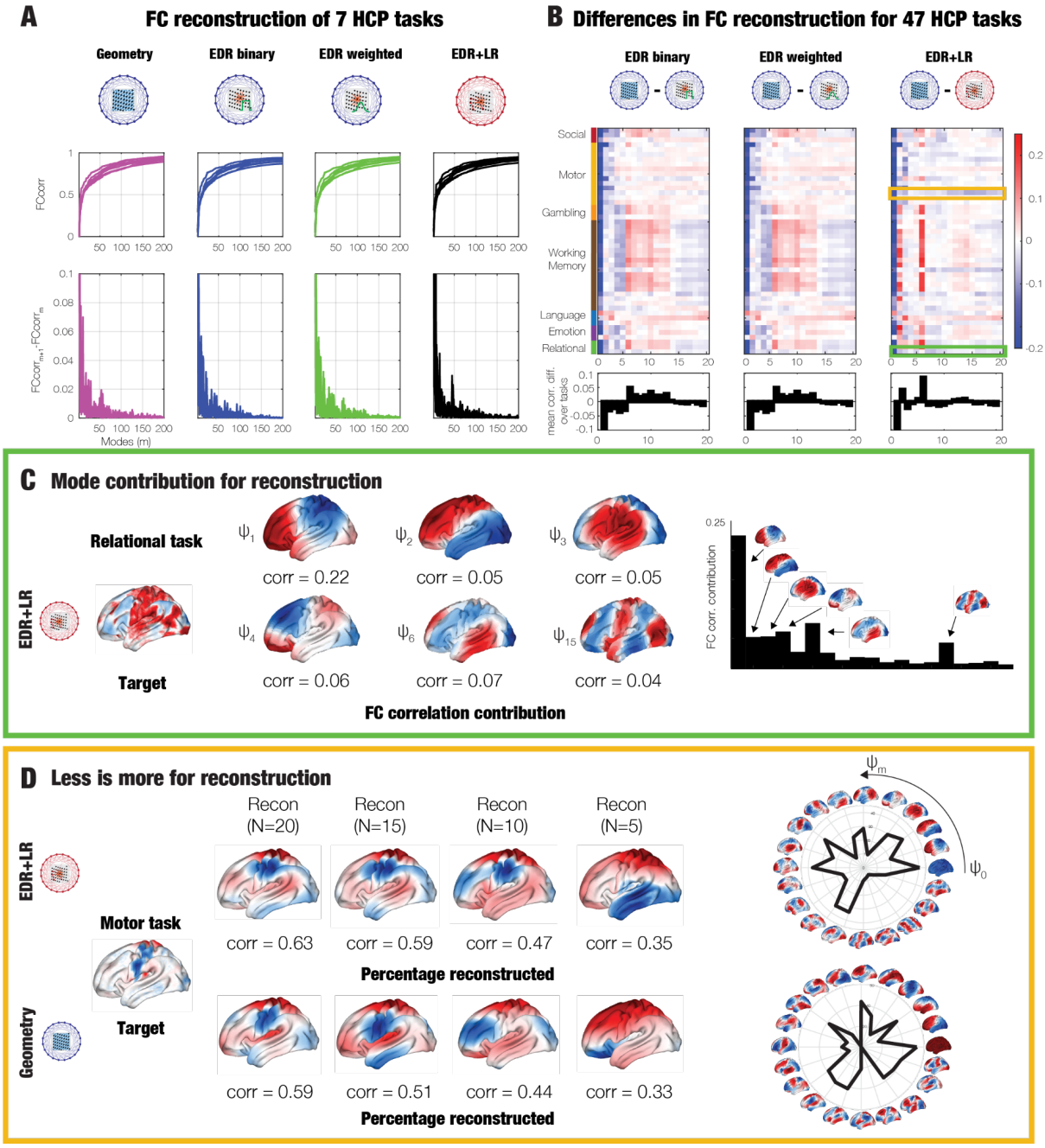

Figure 3. EDR+LR uses fewest harmonic modes to reconstruct task activity. A) For each of four graph representations (top panel) is shown the reconstruction of seven representative activation task fMRI maps. As can be seen, lower frequency modes contribute disproportionately more toward the reconstruction correlation as it can be seen by the elbow around 20 modes (lower panel). **B)** This can also be seen in the reconstruction error for all 47 HCP tasks for the EDR cases, each benchmarked against the geometrical modes for the first 20 modes, where the top panel shows hues of blue with better performance of the EDR modes while red hues mean better performance of the geometric modes. The lower panel shows the average across the 47 HCP tasks. **C)** Individual mode contribution towards the reconstruction

of the relational task. We show the disproportional contribution of some modes (1, 2, 3, 4, 6, 15) to the overall reconstruction, where the brain renderings show the reconstruction to the overall activation map (far left). **D)** Similarly, for the motor task target (far left), we compare the overall correlational contributions of the number of modes (using 20, 15, 10 and 5 modes) when using EDR+LR and geometry as the underlying representations. As can be seen, the reconstruction with EDR+LR converges more quickly for lower modes than geometry, suggesting that less is more .